



Photoelectrochemical Tandem Cell with Bipolar Dye-Sensitized Electrodes for Vectorial Electron Transfer for Water Splitting

Jong Hyeok Park and Allen J. Bard^{*z}

Department of Chemistry and Biochemistry, The University of Texas at Austin, Austin, Texas 78712, USA

Direct water electrolysis was achieved with a novel monolithic photoelectrochemical cell. Bipolar WO₃/Pt and dye-sensitized TiO₂/Pt semiconductor panels, capable of vectorial electron transfer, have been used for water splitting to yield hydrogen and oxygen; light is the only energy input. The hydrogen production efficiency of this tandem cell, based on the short-circuit current, was ~1.9% and the maximum hydrogen production efficiency was ~2.5% when 0.2 V positive bias was applied. When a concentrated LiCl aqueous solution was used as an electrolyte, valuable chlorine was obtained instead of oxygen. The maximum yielding efficiency of hydrogen and chlorine was ~1.8%.

© 2005 The Electrochemical Society. [DOI: 10.1149/1.2140497] All rights reserved.

Manuscript submitted August 5, 2005; revised manuscript received October 10, 2005. Available electronically December 12, 2005.

Direct splitting of water into hydrogen and oxygen by solar light in photoelectrochemical cells (PECs) has received much attention, since hydrogen is often considered the energy storage medium of the next generation.¹⁻³ Various photoelectrochemical approaches have been introduced for evolving hydrogen directly from sunlight and water, and offer the possibility of increasing the efficiency of the solar-to-hydrogen pathway.^{4,5} Although tandem cells based on III/V semiconductors have achieved high efficiencies, in the range of 12 to ~20%, these single-crystal materials are too expensive for large-area terrestrial applications.^{5,6} Therefore, the main target in recent studies on solar energy conversion is to reduce the fabrication cost while maintaining reasonable conversion efficiency.

Various inexpensive approaches using semiconductor/electrolyte junctions have been proposed, since the pioneering work by Fujishima and Honda,⁷ but so far the conversion efficiency reported still remains quite low (<1%). Recently, Yamada and co-workers demonstrated a device that integrates an amorphous silicon triple-junction solar cell coated with thin film catalysts for the hydrogen and oxygen evolution reaction operating at 2.5% efficiency.⁸ More recently, a new hybrid silicon/photoelectrochemical multijunction cell with 2.2% efficiency was reported.⁹ However, the structure of the silicon-based tandem cell with a multilayer p-i-n junction is complicated. The Grätzel and Augustynski groups have described a low-cost tandem device, based on two photosystems (WO₃ and a dye-sensitized solar cell) connected externally in series that achieved direct water splitting into hydrogen and oxygen by UV-visible light.¹⁰⁻¹² The primary disadvantage of this system is the need for external wiring to connect the WO₃ film electrode to a separate dye-sensitized solar cell (DSSC) based on nanoparticulate TiO₂. Nevertheless, the tandem cell scheme using nanocrystalline WO₃ and a DSSC is an interesting candidate for a low cost water splitting system.

We describe here a water splitting cell using bipolar WO₃/Pt and dye-sensitized TiO₂/Pt electrodes capable of vectorial electron transfer. Our group previously described the use of a series array of bipolar photoelectrodes capable of vectorial electron transfer.¹³⁻¹⁵ Two bipolar electrodes were connected by the iodide/iodine couple in MeCN for the internal connections and can permit unassisted photolytic water splitting with oxygen evolved at the WO₃ semiconductor surface and hydrogen evolved on a platinum surface (Fig. 1a). This device is different than the previously reported tandem cell by the Grätzel group in that the external wiring between the photoelectrochemical cells has been replaced by internal vectorial electron transfer resulting in a monolithic water splitting device. We have also introduced photocatalytic behavior of the WO₃ photoanode to offer specificity in Cl₂ production for the first time. Figure 2 shows

the energetics of vectorial electron transfer from one bipolar photoelectrode to the other. The scheme consists of two photons required to produce one separated electron-hole pair.

Experimental

Peroxytungstic acid sol (WO_{3-x}·H₂O) was synthesized by dissolving tungsten powder (1 g) in an ice-cooled beaker containing a 30% H₂O₂ aqueous solution (5 mL) and then diluting the solution with a water/2-propanol mixture (volume ratio: 5:2).¹⁶ The WO₃ was deposited on a mechanically polished Ti substrate by electrophoresis (-430 mV vs Ag/AgCl, with a Pt mesh counter electrode) from this solution for 30 min and then annealed in air at 450°C for 30 min. The thickness of WO₃ was controlled by consecutive electrodeposition steps, each followed by a heat-treatment. The photoelectrochemical measurements were carried out in a three-electrode system, by illumination with a 2500 W xenon lamp from which infrared wavelengths were removed by an 8-in. water filter. The measured light irradiance was ~100 mW/cm². The potential of the WO₃ electrode was monitored vs an Ag/AgCl reference electrode in 0.25 M Na₂SO₄ acidified to pH 4.0 with perchloric acid.

To characterize the photocurrent characteristics of the DSSC a 15-nm-thick platinum film was deposited onto one side of a 0.25-mm-thick Ti foil (Aldrich, area: 0.12 cm²) by sputtering. A ~15-μm-thick film of TiO₂ nanoparticles (Konarka Corr., Lowell, MA) was printed on another Ti foil. After sintering at 450°C for 30 min and cooling to 80°C, the TiO₂-coated Ti foil was dye-coated by immersing it in a 0.3 mM solution of the Ru-dye Z-907 (Konarka) in acetonitrile and *t*-butanol (volume ratio 1:1) at room temperature for 24 h. Both the WO₃/Pt and DSSC/Pt electrodes were inserted into a Pyrex glass tube and attached with curable epoxy (Devcon Co.) resin at about a 45° angle, with a spacing of 1 cm, to allow irradiation of the photoactive sides of the electrodes. An iodide/iodine-containing electrolyte (0.005 M I₂ + 0.5 M LiI + 0.58 M *t*-butylpyridine in MeCN) filled the Pyrex tube to connect electrolytically the internal faces of the two bipolar electrodes.

Results and Discussion

Because the photocurrent of tandem cells will be limited by the lowest-current cell, current-matching in the component cells is critical for good performance. Therefore, we optimized the photocurrent density of the WO₃ film coated on a mechanically polished Ti substrate by photoelectrochemical studies of this electrode alone.

Photocurrents of the WO₃/Ti foil electrodes with different film thicknesses, controlled by the number of deposition steps, are shown in Fig. 3a. The dark current in the potential region -0.2 to 0.6 V was negligible. The photocurrent onset occurred at about -0.1 V. The onset shifted slightly negatively with increasing light intensity. Each curve showed an increase in photocurrent until saturation was reached at ~0.6 V. Under illumination, the saturation photocurrent

* Electrochemical Society Fellow.

^z E-mail: ajbard@mail.utexas.edu

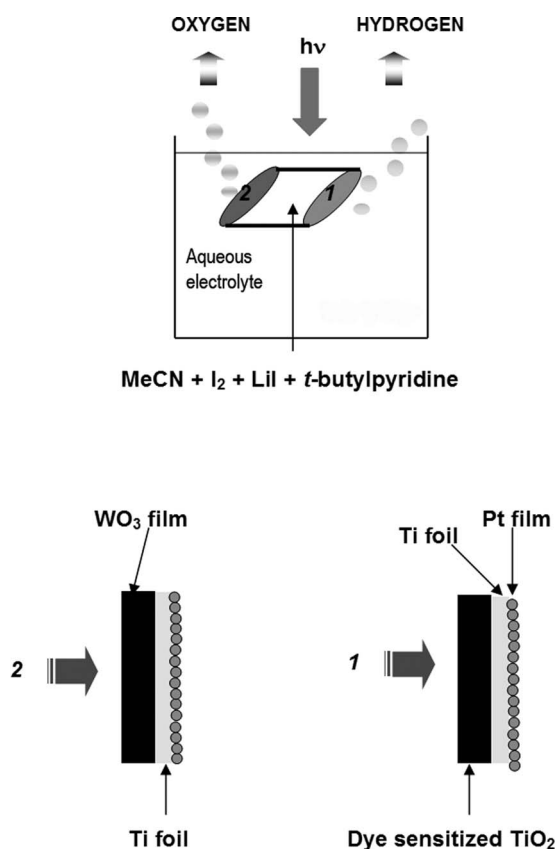


Figure 1. Schematic of water photoelectrolysis cell.

associated with the photogeneration of oxygen reached $\sim 3.7 \text{ mA/cm}^2$.¹¹ There were no significant pH changes in the bulk electrolyte during the photoelectrochemical tests.

In Fig. 3b we show the photocurrent vs voltage characteristics of the DSSC (Pt-coated Ti foil/1-cm-electrolyte/dye-sensitized TiO_2 -coated Ti foil) measured at different incident light intensities. The fill factor (FF) of the device was ~ 0.5 at 100 mW/cm^2 . Moreover, the open-circuit voltage, V_{OC} , and short-circuit current density, i_{SC} , increased monotonically, reaching maximum values of $V_{\text{OC}} = 0.61$ and $i_{\text{SC}} = 9 \text{ mA/cm}^2$, respectively.

Because this tandem cell requires two photons to produce one electron in the external circuit, great care must be taken in each cell to match the photocurrent. For the water splitting experiment, we adjusted the photocurrent density by controlling the areas of the WO_3 photoelectrode and the dye-sensitized TiO_2 photoelectrode.

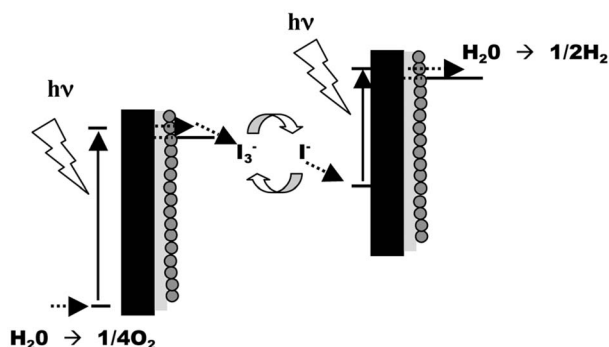


Figure 2. Energy level diagram for the photoelectrochemical water splitting device.

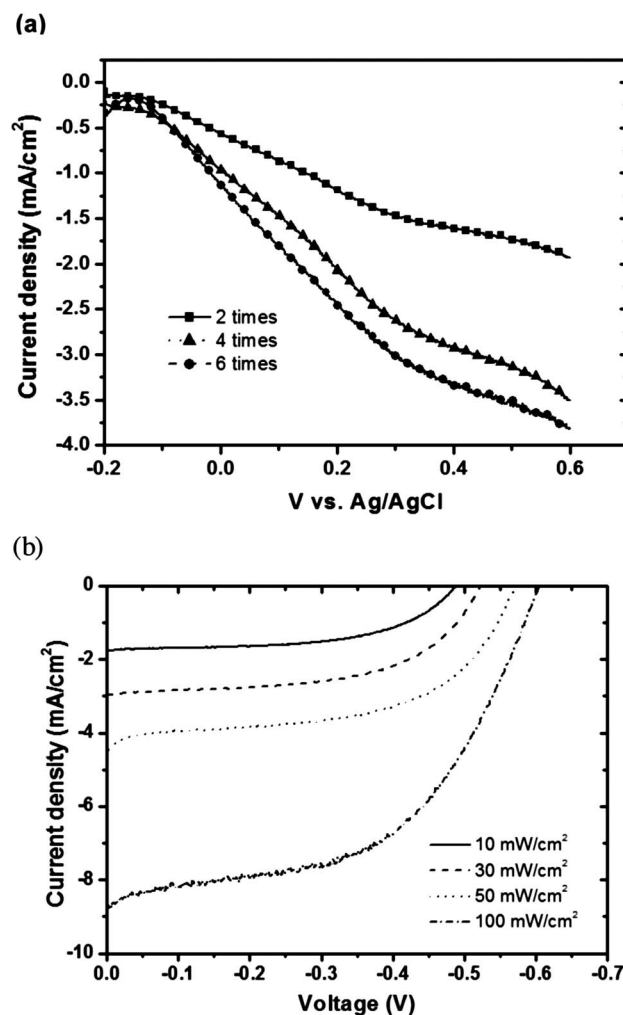


Figure 3. (a) Photocurrent-potential plots for WO_3 electrodes illuminated at 100 mW/cm^2 with a xenon lamp, solution, $0.2 \text{ M Na}_2\text{SO}_4$ (pH 4). (b) Photocurrent behavior of inner DSSC as a function of light intensity.

The ultimate aim of a solar energy storage system would be to photosynthesize an energy-rich chemical (e.g., H_2 from H_2O) without the application of any external bias voltage. As can be seen in Fig. 3a, the system constructed with WO_3 as the photoanode has useful properties, although the wide bandgap of this material (2.8 eV) precludes efficient utilization of the solar spectrum. To obtain solar-to-hydrogen conversion efficiency, the cell was placed in a water jacket as shown in Fig. 1a. For the purpose of performance analysis, the PEC and photovoltaic components of the device can be separated, as illustrated in the inset of Fig. 4a. In the two-electrode configuration, the working electrode is a tandem cell (the back face of 1 was coated with an insulating polymer layer and the working electrode lead was connected to 1) and the counter and reference electrode leads were connected to a Pt plate electrode. This displaces, for measurement purposes, the Pt cathode to one where the current could be monitored. Under illumination, electrons flow from WO_3 to the right of the tandem cell, oxidizing water and generating oxygen. Electrons flow to the DSSC and pass through the external circuit to the Pt plate electrode.

Although the tandem cell has the proper bandgap for water splitting, its bandedges should be adjusted to produce hydrogen and oxygen simultaneously. The band positions of water oxidation and reduction can be easily tuned by adjusting the electrolyte pH. For water splitting experiments, two kinds of electrolytes with different pH values were investigated. Figure 4a shows the bias voltage de-

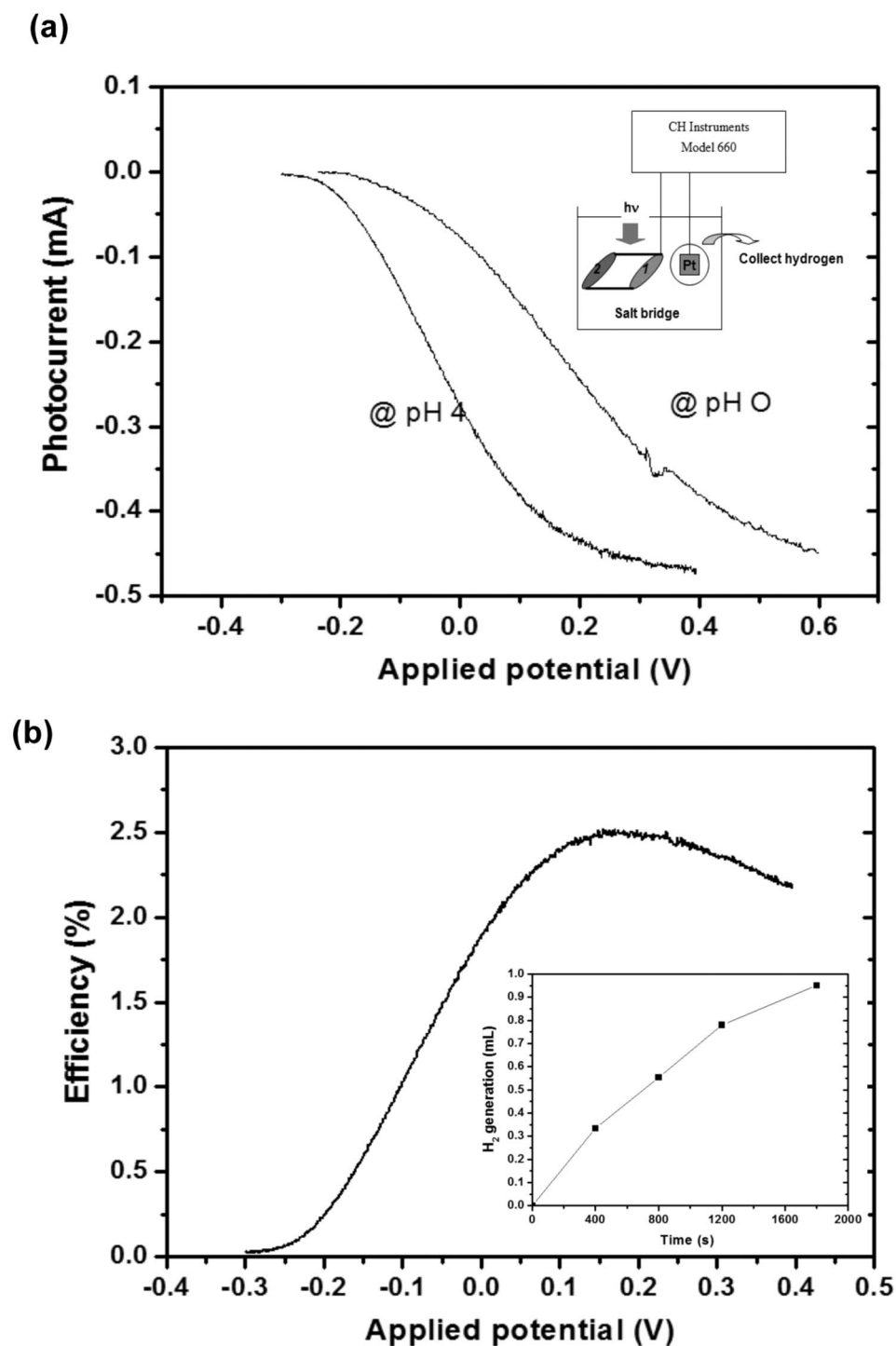


Figure 4. (a) Current density-voltage characteristics for PEC tandem cells connected by either 1 M HClO₄ (pH 0) or 0.25 M Na₂SO₄ + HClO₄ (pH 4) under white light illumination (total area: 0.18 cm²). Inset shows schematic of the two-compartment electrochemical cell for measuring photocurrent in the photoelectrolysis cell. (b) The solar-to-hydrogen conversion efficiency as a function of applied potential. Inset shows hydrogen production from the tandem cell at the open-circuit state under 200 mW/cm² 0.25 M Na₂SO₄ (pH 4) electrolyte.

pendence of the photocurrent of the tandem cell under illumination. The tandem cell in pH 4 electrolyte started to generate hydrogen at a voltage 0.2 V negative of 0 V bias, indicating that no additional external voltage was needed for this tandem cell to split water. The light-limiting current was reached at a positive bias (~ 0.3 V) and remained almost constant with increasing bias. The zero bias point represents the maximum short-circuit photocurrent for water splitting and is the operating point for the cell in photoelectrolysis mode. This current is a result of a combination of the voltage the cell is generating and the voltage needed for water splitting at that photocurrent density.¹⁷ As can be seen in Fig. 4a, the plateau was reached at ~ 0.2 V past the zero bias point. The tandem cell operating at pH

0 started to generate hydrogen at ~ 0 V bias and reached saturated photocurrent at ~ 0.6 V, indicating that additional external voltage was needed for efficient water splitting under these conditions. The better performance at pH 4, compared to pH 0, suggests that improving the kinetics of water oxidation at WO₃ is more important than that of H₂ evolution at Pt. This suggests that even more alkaline electrolytes would be beneficial. However, the WO₃ is not stable under illumination at pHs above 5.

The chemical efficiency during hydrogen production was calculated with the following equation: efficiency = (power out)/(power in). The input power is the incident light intensity of

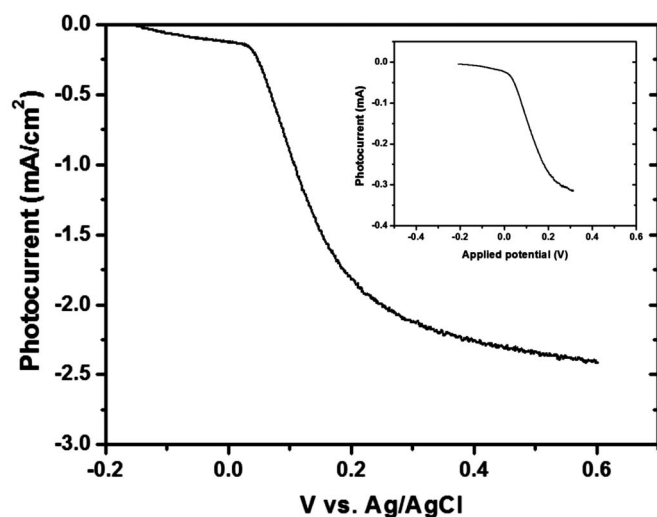


Figure 5. Photocurrent-potential plots for WO_3 electrodes with 2 nm Pt catalyst illuminated with a 100 mW/cm^2 xenon lamp in 15 M LiCl (pH 4). Inset shows current density-voltage characteristics for PEC tandem cells connected by 15 M LiCl (pH 4) under white light illumination (total area: 0.18 cm^2).

100 mW/cm^2 . An ideal tandem cell would operate under short-circuit conditions. Figure 4a results from the combination of photo-voltaic cell characteristics (I_{SC}, V_{OC}, FF) and electrochemical load to produce hydrogen and oxygen. For the output power, assuming 100% photocurrent electrolysis efficiency, the hydrogen production photocurrent of $0.28 \text{ mA}/(\text{total exposed cell area: } 0.18 \text{ cm}^2)$ at zero bias is multiplied by 1.23 V, which is the ideal fuel cell limit at 25°C .⁵ Using this equation, the hydrogen production efficiency of our system at zero bias was 1.9%. The hydrogen conversion efficiency as a function of potential is shown in Fig. 4b. The maximum conversion efficiency was 2.5% and observed at about 0.2 V positive bias [efficiency = photocurrent at 0.2 V \times (1.23 – 0.2)/ 100 mW/cm^2]. The inset of Fig. 4b shows a quantitative description of the hydrogen evolution under zero bias as a function of time. For this test, a larger glass tube, with a 1 cm^2 larger area and photoelectrodes were used. During 1800 s of exposure to 200 mW/cm^2 xenon lamp illumination, $\sim 1 \text{ mL}$ of hydrogen gas was generated.

Figure 5 illustrates a typical current-voltage curve for WO_3 photoanodes with a 2 nm Pt catalyst in contact with 15 M LiCl electrolyte (pH 4). The potential to oxidize Cl^- is 0.36 V higher than that for water oxidation at this pH, however the heterogeneous electron transfer rate for Cl^- oxidation is more favorable. To provide an even greater kinetic advantage for oxidation of Cl^- , an electrolyte with a high concentration of Cl^- was used. The onset potential was similar

to O_2 evolution. However, a sharp increase in current density was observed at about 0.05 V. The Cl_2 gas was identified by its smell and by chemical analysis (oxidation of *N,N*-diethyl-*p*-phenylenediamine indicator by free chlorine). However, the WO_3 photoanode showed lower current density for Cl_2 evolution than for O_2 evolution. This might be caused by some blocking of the input light source by the thin Pt catalyst. The inset of Fig. 5 shows the bias voltage dependence of the photocurrent of the tandem cell under illumination. Under small external bias, the tandem cell produces H_2 and Cl_2 simultaneously. More details of this system are under investigation.

Conclusions

We have demonstrated a tandem photoelectrochemical cell with vectorial electron transfer for water splitting, leading to an unassisted and monolithic system. Water can be split into hydrogen and oxygen using the $\text{WO}_3/\text{DSSC}/\text{Pt}$ device, with light as the only energy input. Because a $\sim 10.4\%$ light-to-electricity conversion efficiency has been obtained for DSSC, novel metal-oxides need to be developed to achieve high solar-to-hydrogen conversion efficiencies. The new electrophoretically deposited WO_3 films on Ti foil show a high photocurrent compared to other WO_3 preparations resulting in a 2.5% maximum solar-to-hydrogen conversion efficiency (under 0.15 V externally applied bias).

Acknowledgments

Support of this research by the National Science Foundation (CHE 0202136) is gratefully acknowledged. We thank Konarka Technology, Inc., for TiO_2 and Z-907. This work was partially supported by the Korea Research Foundation grant (KRF-2004-214-D00266).

References

1. G. R. Torres, T. Lindgren, J. Lu, C. G. Granqvist, and S. E. Lindquist, *J. Phys. Chem. B*, **108**, 5995 (2004).
2. A. J. Bard and M. A. Fox, *Acc. Chem. Res.*, **28**, 141 (1995).
3. A. J. Bard, *Science*, **207**, 139 (1980).
4. S. Licht, *J. Phys. Chem.*, **105**, 6281 (2001).
5. O. Khaselev and J. A. Turner, *Science*, **280**, 425 (1998).
6. M. Grätzel, *Nature (London)*, **414**, 338 (2001).
7. A. Fujishima and K. Honda, *Nature (London)*, **238**, 37 (1972).
8. Y. Yamada, N. Matsuki, T. Ohmori, H. Kondo, A. Matsuda, and E. Suzuki, *Int. J. Hydrogen Energy*, **28**, 1167 (2003).
9. E. L. Miller, B. Marsen, D. Paluselli, and R. Rocheleau, *Electrochem. Solid-State Lett.*, **8**, A247 (2005).
10. M. Grätzel, *Calcif. Tissue Res.*, **3**, 3 (1999).
11. C. Santato, M. Ulmann, and J. Augustynski, *J. Phys. Chem. B*, **105**, 936 (2001).
12. C. Santato, M. Ulmann, and J. Augustynski, *Adv. Mater. (Weinheim, Ger.)* **13**, 511, (2001); **13**, 936 (2001).
13. E. S. Smotkin, A. J. Bard, A. Campion, M. A. Fox, T. Mallouk, S. E. Webber, and J. M. White, *J. Phys. Chem.*, **90**, 4604 (1986).
14. E. S. Smotkin, S. C. March, A. J. Bard, A. Campion, M. A. Fox, T. Mallouk, S. E. Webber, and J. M. White, *J. Phys. Chem.*, **91**, 6 (1987).
15. J. H. Park and A. J. Bard, *Electrochem. Solid-State Lett.* **8**, G371 (2005).
16. P. K. Shen and A. C. C. Tseung, *J. Mater. Chem.*, **2**, 1141 (1992).
17. X. Gao, S. Kocha, A. J. Frank, and J. A. Turner, *Int. J. Hydrogen Energy*, **24**, 319 (1999).